Carolin Hessinger*, Frank Hübner*, Martin Schüßler, Markus Paravicini, Markus Ketomäki, Thomas Vogl and Rolf Jakoby

Evolution of a theranostic applicator for microwave ablation treatment

https://doi.org/10.1515/freq-2022-0088
Received April 25, 2022; accepted June 30, 2022;
published online August 17, 2022

Abstract: The purpose of this work is to further develop a novel dual-mode microwave applicator for diagnosis and thermal ablation treatment. The MR-compatible MW applicator enables differentiation of tumor tissue and healthy tissue through dielectric contrast measurements, optimizing the positioning of the applicator in the lesion. Due to the robust applicator design and the resulting permittivity tracking during ablation, even carbonized tissue can be detected. The use of operating frequencies between 5 and 10 GHz allow a noticeably lower power consumption for microwave ablation of only 20 W compared to commercially available applicators. Clinically relevant dimensions of ablation zones can be achieved and additionally monitored using MR imaging and thermometry.

Keywords: dual-mode microwave applicator; liver cancer; microwave ablation; multimodality imaging; theranostic.

1 Introduction

Microwave technology and techniques offer novel treatment options as well as diagnostic tools for medicine. The electromagnetic field with frequencies in the microwave range between 300 MHz and 300 GHz interacts with organic tissue in a non-contact and non-destructive way. From this interaction, information about the tissue type and its constitution can be extracted. Further, by increasing the excitation power, heating or even destruction of the tissue can be achieved. Microwave ablation (MWA) uses this phenomenon to destroy tumors with heat. During the minimally invasive procedure, a needle-shaped antenna (active part of the applicator) is guided through the patient's body towards the targeted lesion which is then destroyed via heat. Even though surgical resection of tumors is still the gold standard in the treatment of many solid tumors in the liver, the number of inoperable tumors is large. For example, when the tumor has grown in a difficult-to-reach body area, near a major blood vessel or other critical structures, of the organ. For these cases, minimally invasive treatment options are effective alternatives. The advantages are much shorter treatment duration as well as faster convalescence and lower risks of infections. Moreover, a recent study demonstrated that MWA enables a significant reduction of circulating tumor cells in patients with hepatocellular carcinoma (HCC) (tumoricidal effect) [1].

The current aim of microwave ablation systems as minimal-invasive solutions is to provide a curative treatment option instead of being applied only as palliative care. Curative in this sense means that the increase of the therapeutic temperature above 60 °C in the targeted tissue can be monitored and controlled, allowing for a localized heating and a complete coagulation and destruction of the tumor plus a security margin of about 5 to 10 mm of the healthy surrounding tissue. Up to now, data on performance and duration of commercially available ablation therapy systems have been summarized in tables by the manufacturers of the respective probes and are based on clinical studies with ex vivo and/or *in vivo* experiments. This data is not standardized and does not include patient-specific characteristics that might be important for an optimal ablation performance [2, 3]. In addition, for a precise tumor localization as well as a more efficient destruction of tumor cells and a better protection of healthy surrounding tissue, i.e. preventing undertreatment or overtreatment, a real-time non-invasive imaging is essential [4]. Generally, in the percutaneous procedures, ultrasound (US), computed

Carolin Hessinger and **Frank Hübner** contributed equally.

***Corresponding authors: Carolin Hessinger**, Institute for Microwave Engineering and Photonics, Technische Universität Darmstadt, Merckstr. 25, 64283 Darmstadt, Germany, E-mail: reimann@imp.tu-darmstadt.de; **Frank Hübner,** Institute of Diagnostic and Interventional Radiology, J. W. Goethe-Universität Frankfurt, Theodor-Stern-Kai 7, 60590, Frankfurt am Main, Germany, E-mail: frank.huebner@kgu.de
Martin Schüßler, Markus Paravicini and Rolf Jakoby, Institute for Microwave Engineering and Photonics, Technische Universität Darmstadt, Merckstr. 25, 64283 Darmstadt, Germany
Markus Ketomäki and Thomas Vogl, Institute of Diagnostic and Interventional Radiology, J. W. Goethe-Universität Frankfurt, Theodor-Stern-Kai 7, 60590, Frankfurt am Main, Germany

tomography (CT) or magnetic resonance imaging (MRI) can be employed for targeting the tumor tissue and controlling the ablation process. MRI is non-invasive, avoids ionizing radiation, provides a multi-directional image acquisition with a high contrast and resolution and allows for an online thermometry [5]. Current microwave ablation procedures are performed under CT guidance that has several disadvantages compared to MRI due to the ionizing radiation and less accurate imaging.

In this article, a multimodality approach is presented which can be realized by combining the MR imaging and MRI thermometry with a microwave sensor integrated at the tip of the microwave applicator. In combination with a dedicated calibration procedure, it provides accurate and real-time information to position the needle-like device into tumorous tissue (Figure 1). Once the applicator is inserted into the targeted tumor, the sensing mode could also be used during the thermal ablation treatment to monitor temperature changes by detecting the specific permittivity drop that occurs when a temperature above 60 °C is achieved. Hence, the dual-mode applicator is used not only for therapy but also for diagnostics (theranostics). Together with MRI thermometry, the proposed dual-mode microwave ablation system gives detailed information in the applicator's vicinity as well as overall information of the temperature distribution in the tissue.

To date, there are only a few approaches that use the detection of changes in the dielectric properties of the tissue to represent and regulate the course of treatment of MWA. The general feasibility of a microwave tomography system as treatment monitoring option was evaluated in [6]. The concept was further evaluated in-silico underlining the potential of using microwaves as fast and non-invasive way to observe the therapy progress [7]. Another approach utilizing dielectric differences between tumorous, normal and ablated tissue, is given in [8]. The method is based on the evaluation of the broadband reflection signal of the microwave applicator in the time domain to determine the tumor-normal tissue boundary. The required a-priori knowledge of the dielectric properties of the tissue surrounding the applicator is obtained by a further method proposed by the same group [9].

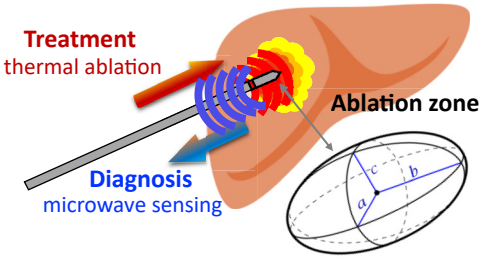

Figure 1: Dual-mode concept based on two operational modes to detect tumors and perform thermal ablation.

In contrast to the presented approaches of microwave-based monitoring of treatment progress, the dual-mode concept is deliberately designed as complementary imaging to MRI by serving as an additional source of information to increase treatment success rather than substituting already established imaging techniques.

2 Preliminary investigations

The feasibility of a microwave applicator with sensing properties to detect tumor tissue is strongly dependent on the question whether normal and tumor tissue be distinguished by microwaves. To answer this, a clinical study was performed to determine the patient-specific dielectric contrasts of freshly resected ex-vivo human liver samples [10]. According to those results, sensitivity requirements for novel MWA systems for tumor detection can be formulated. The clinical study included measurements of the complex permittivity of five liver samples consisting of tumorous and healthy tissue in the frequency range between 0.5 and 26.5 GHz. In Figure 2 the mean values and corresponding standard deviations of the real and imaginary parts of the measured relative permittivity at 5.8 GHz of each patient are shown. As described in [10] the observed permittivity trend at 2.45 GHz is very similar. The discrete frequencies at 2.45 and 5.8 GHz are in ISM bands (Industrial, Scientific, and Medical Bands) and represent a current and a possible future working frequency of MWA systems. In general, the contrast between healthy and tumorous tissue is higher than the corresponding standard deviation. Hence, a distinction between healthy and tumor tissue would be possible. Only patient 3 shows a larger standard deviation of the measurement points in the healthy tissue. A possible explanation for this could be the scattering of tumor cells into the tissue declared as healthy. Further, the frequency-dependency of the patient-specific dielectric contrast was evaluated. It varies strongly from patient to patient with maximal dielectric contrast between 28.9% (patient 3) and 60.9% (patient 2) and local maxima in the frequency range between 8 and 12 GHz.

According to the results of this study, dielectric contrast measurements yield the possibility to detect the presence of tumor tissue in contrast to healthy tissue. However, those measurements must be performed individually per patient. For the feasibility of microwave-based detection systems, it could thus be deduced that the application of general data sheets with threshold values

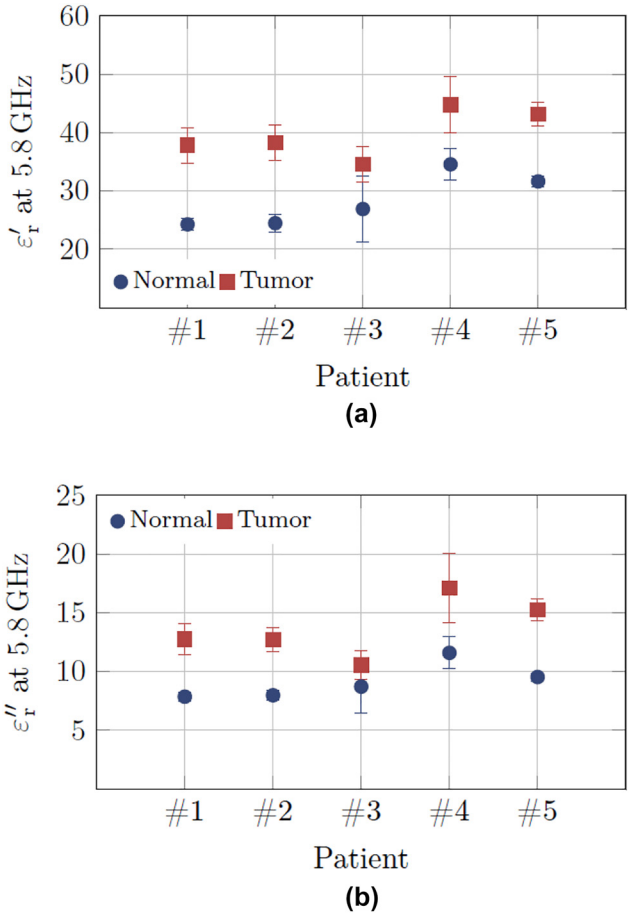

Figure 2: The mean value and standard deviation of (a) real and (b) imaginary part of the complex permittivity of normal and tumor liver tissue at 5.8 GHz [10].

for the differentiation between healthy and tumor tissue are not practicable. Instead, individual measurement of dielectric contrast should be performed for tumor detection. In terms of sensitivity requirements of microwave-based detection devices, dielectric contrasts in the range of 20% should be resolved. Therefore, the corresponding extraction error should be smaller than ±10%.

3 Applicator development

For the applicator design an open-ended coaxial slot geometry was selected. The geometry is further extended by a blocking structure to reduce backward traveling waves that could lead to burning of the healthy tissue around the operating channel. Further, backward traveling waves could influence the shape of the ablation zone towards more longitudinal extended lesions that would not meet the rather spherical shaped tumor sizes. The relevant design parameter of the structure are the distance between the open end and slot, the length of the slot, the distance from the slot to the blocking structure and the length of the blocking structure. The resonance frequency is dominantly determined by the distance between slot and open end of the coaxial cable that corresponds to a quarter wavelength of the guided wave at resonance frequency. A standing wave between the distal end and the slot of applicator is created with an electrical field minimum and an induced current maximum in the position of the slot. Hence, the slot is equivalent to a quarter wave monopole feeding point where the maximum radiation occurs. The axial and radial cross sections of the geometry and relevant design parameters are given in Figure 3.

The applicator development process was performed in an iterative way. First, a prototype based on a UT 085 coaxial cable with a diameter $Ø_{out}$ = 2.1 mm was designed. The applicator operated in the frequency range between 5 and 7 GHz for complex permittivity extraction and the thermal ablation was performed at an operating frequency of 5.8 GHz [11]. In a second step, the applicator was further optimized by a decrease of the coaxial cable diameter to $Ø_{out}$ = 1.19 mm in order to reduce the invasiveness of the needle-like tool. The geometrical parameters of the structure were determined by full-wave simulation, taking into account biological and temperature-dependent material properties of the environment. A multi objective optimization of the geometrical parameters of the coaxial slot

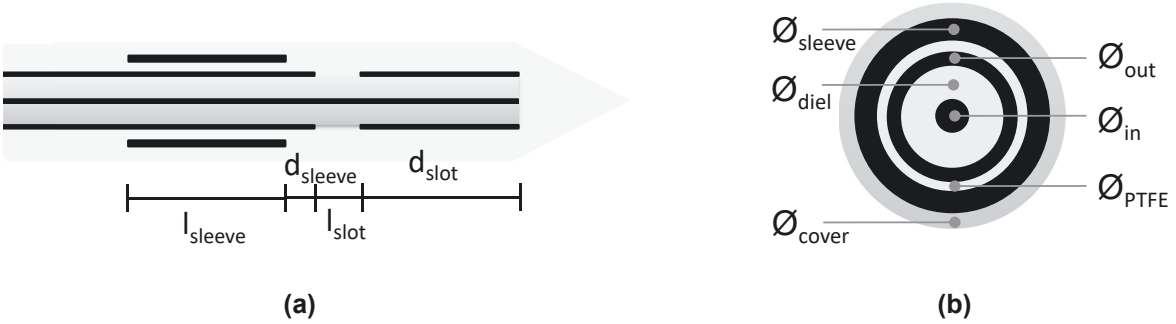

Figure 3: Applicator design. (a) Axial and (b) radial cross section of open-ended coaxial slot applicator with relevant geometric parameters.

structure was performed based on a mulit physical approach incorporating electromagnetic-thermal coupled simulations [12]. The optimization objectives were a maximized applicator efficiency and ablation zone characteristics in terms of spherical shape and maximum size. As constraint of the optimization, the sensing sensitivity of the coaxial slot applicator is taken into account as a key factor that must be fulfilled for the dual-mode functionality. The relative permittivity is extracted by means of a three-step calibration procedure based on the well-known open coaxial probe de-embedding method [13]. As described in [11], the equivalent circuit of the open-ended slot applicator at the operating frequency can be transformed in a way that the de-embedding procedure can be applied with a parallel capacitance that is solely dependent of the surrounding complex permittivity of the Material under Test (Figure 4). The relation between the measured reflection coefficient $\underline{\Gamma}_{\text{meas}}$ and the surrounding complex permittivity is bilinear and can be described by following equation.

$$\underline{\varepsilon}_r = \frac{\underline{a}\,\underline{\Gamma}_{\text{meas}} + \underline{b}}{\underline{c}\,\underline{\Gamma}_{\text{meas}} + 1},$$

with $\underline{a}$, $\underline{b}$, and $\underline{c}$ as complex coefficient that are determined by three measurements with calibration standard material with known permittivity. As reference materials, saline solution with various sodium chloride (NaCl)- concentrations were used. Those substances are easy and cost-efficient to fabricate and provide well-known material properties that are in the range of organic tissue dielectric properties.

For the optimizing of the geometric parameters of the open-ended coaxial slot applicator, the sensitivity was evaluated by determining the extracted relative permittivity values and compare it to the actual simulated values. By this procedure, the applicators performance is considered also for simulations with reference materials. The resonance frequency of the optimized structure inserted into liver tissue is not exactly at the operating frequency of 5.8 GHz but shifted towards a lower frequency at 5.4 GHz (Figure 5). For the case when the applicator is inserted into deionized water (DIW) with different dielectric properties compared to liver tissue, the matching is still very good below –15 dB. Hence, the sensitivity analysis as constraint for the optimization procedure could be considered as method for a robust applicator design that is not so prone to permittivity changes in the surrounding such as they occur during an ablation procedure. Reflection coefficient measurements of a fabricated optimized prototype with a diameter of $\text{Ø}_{\text{out}} = 1.19$ mm inserted into DIW are in good agreement with the simulations as shown in Figure 5.

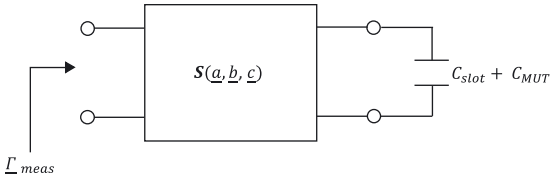

Figure 4: Simplified two port network of the open ended coaxial slot applicator. Transmission characteristics that are not dependent of the surrounding dielectric properties are included in the two port described by the matrix *S*.

4 Results

The sensing mode and ablation performance of the dual-mode applicator prototypes were systematically analyzed via simulations and measurements. Furthermore, the MRI compatibility of the applicator itself in a non-active state as well as in operation of the sensing mode was evaluated. In the following, the results are summarized.

4.1 Sensing mode evaluation

In [11], a sensitivity analysis of the prototype applicator with a diameter $\text{Ø}_{\text{out}} = 2.1$ mm inserted into various saline solutions and DIW with known permittivity values is described that yielded a mean extraction error of less than 5%. With this accuracy, the dielectric contrast between healthy and tumor liver tissue could be resolved. In a next step the feasibility of extracting dielectric properties during an ablation procedure was evaluated. With the temperature change of the tissue, the relative permittivity decreases. In the case when carbonization occurs, a sudden permittivity drop can be observed [14, 15]. Figure 6 shows the measured permittivity curves as a function of

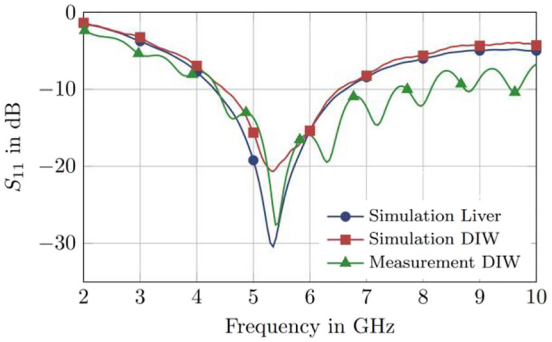

Figure 5: Reflection coefficient simulation of applicator inserted into liver tissue and DIW and measurement of a fabricated applicator inserted into DIW.

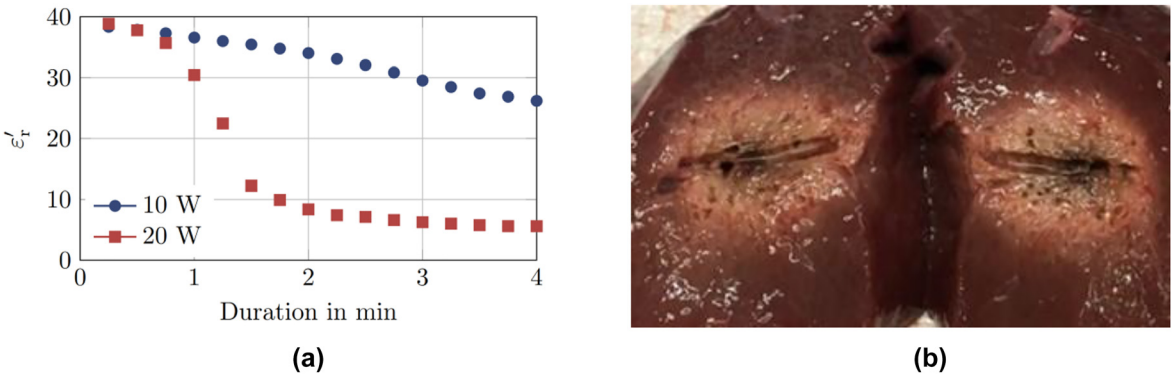

Figure 6: Sensing mode evaluation. (a) Relative permittivity measurement during an ablation with an input power of 10 W (blue) and 20 W (red). The tissue carbonization can be detected during the intervention and was confirmed by (b) a visual control of the ablated tissue sample.

time of ablations with ex vivo bovine liver with an input power of 10 and 20 W. During the measurement, due to permittivity tracking during ablation with an input power of 20 W, carbonized tissue could be detected. This was confirmed by visual inspection of the tissue sample following the measurement. This method allows individual assessment of the tissue condition during ablation in the immediate vicinity of the active part of the applicator. Thus, the dual-mode applicator in detection mode could provide initial feedback to assess the individual absorption of microwave energy in the patient's tissue.

4.2 Ablation performance

To systematically evaluate the ablation performance and sphericity of the laboratory demonstrator, ablations were performed at a power of 20 W and an ablation durations of 10 min in an ex vivo porcine liver. The shape of the ablation zone corresponds to a rotationally symmetric ellipsoid with radii $a = c$ and half of the length b, as shown in Figure 1. The ablation volume $V = 4/3\,\pi a^2 b$ of ten ablation experiments and the sphericity index $SI = a/b$ were determined. The results showed a mean ablation volume of $V = 23.34 \pm 4.41$ cm^3 and an SI between 0.60 and 0.66 (Figure 6). With the determined volume, the radii are on average $a = 1.56$ cm and $b = 2.28$ cm, so that the clinically relevant dimensions for the treatment of tumors with a diameter of 2 cm are achieved. However, an approximately spherical ablation zone ($SI = 1$) is desired in interventional oncology therapy because tumors are predominantly spherical in shape. Sphericity could be optimized with increasing frequency [16, 17]. This should be investigated in further studies.

4.3 MRI-compatibility and thermometry

The evaluation of the MRI compatibility of the dual-mode applicator was performed on a demonstrator with a non-magnetic cable of type UT-047C-LL (Elspec GmbH) and a cable diameter of 1.19 mm. Systematic evaluation and classification of image artifacts from interventional needles is significant for the feasibility and efficiency of ablation therapies. MRI artifacts from applicators often show up as signal loss, which can obscure significant structures in the organ (if significant in size). In addition, accurate visualization of the applicator tip is very important, as underestimation of the penetration depth can lead to accidental puncture wounds in the surrounding (healthy) tissue [18]. In contrast, overestimation of the applicator length could potentially lead to insufficient insertion depth and thus reduce therapeutic efficacy [2]. MR imaging was performed *in vitro* on a 1.5 T MR scanner (Magnetom Aera, Siemens Healthineers, Erlangen, Germany). A homogeneous gel phantom of agarose (3.0 wt%) was poured around the applicator to evaluate the image artifacts. MR contrast agent (0.5%, Dotarem, Guerbet GmbH, Sulzbach, Germany) was added to the phantom to enhance contrast in the T1-weighted sequences. Image artifacts were evaluated at different sequence types (T1-weighted and T2-weighted Turbo Spin Echo (TSE), T1-weighted Fast Low Angle Shot (FLASH)) and different applicator angles of attack (0°, 45°, 90°). In the MR images (Figure 7), the artifact diameter at the applicator tip was determined and the tip location error (TLE) was analyzed. Results of the artifact analysis showed a general overestimation of the applicator size and tip position. The applicator induces a mean artifact diameter of 1.95 ± 0.37 mm at the tip. The TLE was determined to be 1.05 ± 0.63 mm. The resulting artifacts are minimal in the context of this work and are below the 5 mm threshold for

MR interventions postulated by Frahm et al. and Wonneberger et al. in terms of artifact diameter and TLE [8, 19].

For the validation of the MRI compatibility of the active dual-mode applicator, measurements of the sensing mode were performed within the MRI (Figure 7). For this purpose, a phantom consisting of three layers with varying dielectric properties was used, through which the applicator is guided during the course of the measurement [20]. During this procedure MR imaging was performed with a TSE sequence used in clinical practice. A picture of the applicator in the phantom during the experiment is given in Figure 8. The permittivity was extracted at ten different positions within the phantom. This corresponds to a distance between two measurement positions of about 1 cm.

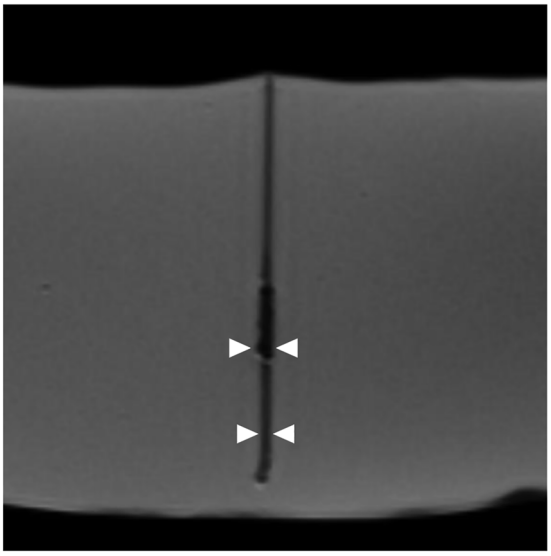

Figure 7: MR imaging of the applicator using T1w-TSE sequence in axial orientation in the gel phantom. The diameter of the artifacts in this image are 3.5 and 2.2 mm respectively (white arrows).

While the first and third layer of the phantom have the same dielectric properties, the middle layer, colored in red, provides a dielectric contrast to represent the scenario of a tumor with a different permittivity compared to the surrounding healthy tissue. Figure 8 gives the contrast values of the two consecutive values of the relative permittivity $|\Delta\varepsilon_r'|$. A jump in permittivity between positions 5 and 6 can be clearly extracted, indicating the different layers of the phantom. This result provides a fundamental evidence that the dielectric properties, in particular the contrast between diseased and healthy tissue is detectable by means of the dual-mode applicator in MRI. In conclusion, it can be deduced from the experiment that when used simultaneously, both the functionality of MRI imaging and that of the dual-mode applicator in detection mode are guaranteed.

As a part of the evaluation of the clinical application of the applicator, MR thermometry was performed in further experiments to check for artifacts and field distortions [5, 21, 22]. An RF-spoiled gradient echo sequence was used to obtain magnitude and phase difference images with the following image parameters: TR = 50 ms, TE = 13 ms, field of view = 220 × 220 mm^2, matrix size = 128 × 128, slice thickness = 7 mm, acquisition time = 2.13 s. Fat suppression was implemented. First, thermometry was performed over a period of 20 min at 4 s intervals in the passive state of the applicator and then in the active detection mode. For this purpose, the gel phantom from the artifact evaluation in imaging was used to obtain a homogeneous medium around the applicator. In each image, a region of interest (ROI) was positioned at a distance of 3 mm from the slot and in the outer region of the phantom to determine the signal-to-noise ratio (SNR). The ROI near the applicator had a size of 3 × 3 pixels and the ROI to determine the image noise at a greater distance from the applicator had a size of

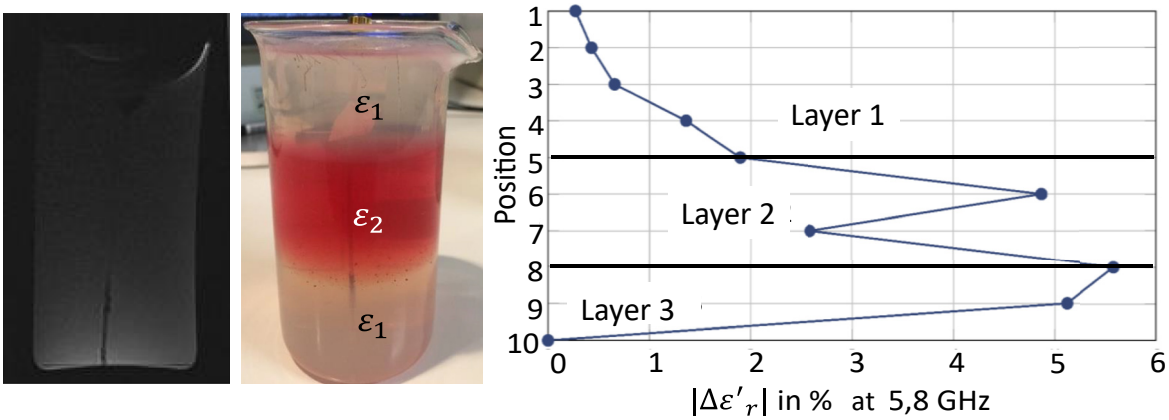

Figure 8: Validation of the detection mode of the applicator during MR measurement in ten different layers in a gel phantom.

6 × 6 pixels. With the detection mode, the SNR was 29.56 ± 2.37 and without the detection mode, the SNR was 30.40 ± 2,60. In comparison, a significance of 0.98 was obtained. Artifacts could not be evidenced during detection. In a second experiment, the applicator was positioned for heating in ex vivo porcine liver tissue. In addition, four fiberoptic temperature probes were positioned in the liver, which were visualized in the transverse MR image. The measured temperature was used for comparison with the calculated temperature at the probe tips. Ablation was performed at 20 W. Over a period of 16 min, ablation was performed intermittently for 25 s, followed by an interruption of 5 s to perform MR thermometry. Using proton resonance frequency (PRF) thermometry, temperatures were calculated over an ROI of 2 × 2 pixels [23, 24]. A comparison of the measured and calculated temperature values showed a slope of m = 1.06 and a correlation coefficient of 1. Artifacts and field distortions could not be proven with the theranostic applicator and is appropriate for use in image-guided ablation procedures.

5 Conclusion and outlook

This work presents the development of a theranostic applicator for clinical use in percutaneous microwave ablation. The results demonstrate the potential of multimodality imaging to improve tumor localization and monitoring during MR-guided MWA. Dielectric contrast measurements can detect tumor tissue in contrast to healthy tissue and optimize the positioning of the applicator. A significant change in permittivity could be demonstrated with the dual-mode applicator in MRI. In the sensitivity analysis of the prototype applicator with a diameter of 2.1 mm, a mean extraction error of less than 5% was obtained. This is noticeably below the sensitivity requirements of microwave-based detection devices, whose dielectric contrast are resolved in the range of 20%. Due to the robust applicator design and resulting permittivity tracking during ablation, carbonized tissue can also be detected. This provides a further option for monitoring interventional oncology therapy in addition to imaging and thermometry. Furthermore, clinically relevant dimensions of ablation zones could be achieved with the prototype applicator at a power of 20 W. In addition, there were minimal artifacts in MR imaging, which are acceptable for applicator positioning and monitoring. MR thermometry can also be used since no field distortions were detected.

In further studies, the sphericity of the ablation zone should be further optimized. Furthermore, a validation of the ablation performance could be performed under additional water cooling of the applicator shaft. Based on the results of this work, the developed dual-mode microwave applicator can be prepared for (pre-) clinical studies in the future.

Acknowledgement: This research is supported by a grant from the German Research Foundation (DFG) in the context of the priority program "ESSENCE" to the project "Dual-mode microwave applicator for diagnosis and thermal ablation treatment of organic tissue" with the reference numbers JA 921/52-2 and VO 479/17-2. Furthermore, the authors would like to thank CST AG for providing CST Microwave Studio software package.

Author contributions: All the authors have accepted responsibility for the entire content of this submitted manuscript and approved submission.

Research funding: None declared.

Conflict of interest statement: The authors declare no conflicts of interest regarding this article.

Ethical approval: For the experiments involving the use of human subjects, an ethical approval with the reference number 321/14 was obtained from the ethics committee of the J.W. Goethe-Universitätsklinikum.

References

[1] T. J. Vogl, L. J. Riegelbauer, E. Oppermann, et al., "Early dynamic changes in circulating tumor cells and prognostic relevance following interventional radiological treatments in patients with hepatocellular carcinoma," *Plos one*, vol. 16, no. 2, p. e0246527, 2021.

[2] D.-E. Kessler, J. Weiss, H. Rempp, et al., "In vitro artifact assessment of an MR-compatible, microwave antenna device for percutaneous tumor ablation with fluoroscopic MRI-sequences," *Minim. Invasive Ther. Allied Technol. MITAT Off. J. Soc. Minim. Invasive Ther.*, vol. 27, no. 1, pp. 60–68, 2018.

[3] F. Hübner, R. Schreiner, C. Reimann, et al., "Ex vivo validation of microwave thermal ablation simulation using different flow coefficients in the porcine liver," *Med. Eng. Phys.*, vol. 66, pp. 56–64, 2019.

[4] T. J. Vogl, N.-E. A. Nour-Eldin, R. M. Hammerstingl, B. Panahi, and N. N. N. Naguib, "Microwave ablation (MWA): basics, technique and results in primary and metastatic liver neoplasms - review article," *ROFO. Fortschr. Geb. Rontgenstr. Nuklearmed.*, vol. 189, no. 11, pp. 1055–1066, 2017.

[5] B. Bazrafshan, F. Hübner, P. Farshid, et al., "Magnetic resonance temperature imaging of laser-induced thermotherapy: assessment of fast sequences in ex vivo porcine liver," *Future Oncol. Lond. Engl.*, vol. 9, no. 7, p. 1039–1050, Jul, 2013.

[6] R. Scapaticci, V. Lopresto, R. Pinto, M. Cavagnaro, and L. Crocco, "Monitoring thermal ablation via microwave tomography: an ex vivo experimental assessment," *Diagn. Basel Switz.*, vol. 8, no. 4, p. E81, 2018.
[7] M. Wang, R. Scapaticci, M. Cavagnaro, and L. Crocco, "Towards a microwave imaging system for continuous monitoring of liver tumor ablation: design and in silico validation of an experimental setup," *Diagnostics*, vol. 11, no. 5, May 2021, Art. no. 5.
[8] U. Wonneberger, B. Schnackenburg, F. Streitparth, T. Walter, J. Rump, and U. K. M. Teichgräber, "Evaluation of magnetic resonance imaging-compatible needles and interactive sequences for musculoskeletal interventions using an open high-field magnetic resonance imaging scanner," *Cardiovasc. Intervent. Radiol.*, vol. 33, no. 2, pp. 346–351, 2010.
[9] V. Lopresto, R. Pinto, L. Farina, and M. Cavagnaro, "Treatment planning in microwave thermal ablation: clinical gaps and recent research advances," *Int. J. Hyperth. Off. J. Eur. Soc. Hyperthermic Oncol. North Am. Hyperth. Group*, vol. 33, no. 1, pp. 83–100, 2017.
[10] C. Hessinger Née Reimann, B. Bazrafshan, F. Hübner, et al., "Dielectric contrast between normal and tumor ex-vivo human liver tissue," *IEEE Access*, vol. 7, pp. 164113–164119, 2019.
[11] C. Hessinger Née Reimann, B. Bazrafshan, M. Schüßler, et al., "A dual-mode coaxial slot applicator for microwave ablation treatment," *IEEE Trans. Microw. Theor. Tech.*, vol. 67, no. 3, pp. 1255–1264, 2019.
[12] C. Hessinger, M. Schüßler, S. Klos, M. Kochanek, and R. Jakoby, "Numerical optimization of an open-ended coaxial slot applicator for the detection and microwave ablation of tumors," *Biology*, vol. 10, no. 9, Sep. 2021, Art. no. 9.
[13] A. Kraszewski, M. A. Stuchly, and S. S. Stuchly, "ANA calibration method for measurements of dielectric properties," *IEEE Trans. Instrum. Meas.*, vol. 32, no. 2, pp. 385–387, 1983.
[14] V. Lopresto, R. Pinto, G. A. Lovisolo, and M. Cavagnaro, "Changes in the dielectric properties of$\less$i$\greater$ex vivo$\less$/i$\greater$bovine liver during microwave thermal ablation at 2.45 GHz," *Phys. Med. Biol.*, vol. 57, no. 8, p. 2309–2327, 2012.
[15] Z. Ji and C. L. Brace, "Expanded modeling of temperature-dependent dielectric properties for microwave thermal ablation," *Phys. Med. Biol.*, vol. 56, no. 16, pp. 5249–5264, 2011.
[16] J. F. Sawicki, J. D. Shea, N. Behdad, and S. C. Hagness, "The impact of frequency on the performance of microwave ablation," *Int. J. Hyperth. Off. J. Eur. Soc. Hyperthermic Oncol. North Am. Hyperth. Group*, vol. 33, no. 1, pp. 61–68, 2017.
[17] C. Hessinger, *Dual-mode mikrowellenapplikatoren für die diagnose und thermische ablation von lebertumoren*, Dissertation Darmstadt, Technische Universität, 2020.
[18] A. Grimm, M. Winkelmann, J. Weiß, et al., "Artefact and ablation performance of an MR-conditional high-power microwave system in bovine livers: an ex vivo study," *Eur. Radiol. Exp.*, vol. 3, no. 1, p. 39, 2019.
[19] C. Frahm, H. B. Gehl, U. H. Melchert, and H. D. Weiss, "Visualization of magnetic resonance-compatible needles at 1.5 and 0.2 Tesla," *Cardiovasc. Intervent. Radiol.*, vol. 19, no. 5, pp. 335–340, 1996.
[20] M. Kochanek, C. Hessinger, M. Schüßler, R. Jakoby, F. Hübner, and T. J. Vogl, "Microwave ablation applicator with tumor detection ability," *IEEE SENSORS*, pp. 1–4, 2020, https://doi.org/10.1109/SENSORS47125.2020.9278609.
[21] F. Hübner, B. Bazrafshan, J. Roland, A. Kickhefel, and T. J. Vogl, "The influence of Nd:YAG laser irradiation on Fluoroptic® temperature measurement: an experimental evaluation," *Laser Med. Sci.*, vol. 28, no. 2, pp. 487–496, 2013.
[22] B. Bazrafshan, F. Hübner, P. Farshid, et al., "Temperature imaging of laser-induced thermotherapy (LITT) by MRI: evaluation of different sequences in phantom," *Laser Med. Sci.*, vol. 29, no. 1, pp. 173–183, 2014.
[23] B. Bazrafshan, A. Koujan, F. Hübner, C. Leithäuser, N. Siedow, and T. J. Vogl, "A thermometry software tool for monitoring laser-induced interstitial thermotherapy," *Biomed. Tech.*, vol. 64, no. 4, pp. 449–457, 2019.
[24] F. Hübner, R. Schreiner, B. Panahi, and T. J. Vogl, "Evaluation of the thermal sensitivity of porcine liver in CT-guided cryoablation: an initial study," *Med. Phys.*, vol. 47, no. 10, pp. 4997–5005, 2020.